Journal of Hydrology: Regional Studies 47 (2023) 101428

Contents lists available at ScienceDirect

Journal of Hydrology: Regional Studies

journal homepage: www.elsevier.com/locate/ejrh

Flooding risk of cropland areas by *repiquetes* in the western Amazon basin: A case study of Peruvian Tamshiyacu City

Jonathan Valenzuela [a,b,*], Manuel Figueroa [a,b], Elisa Armijos [a,b], Jhan-Carlo Espinoza [c], Sly Wongchuig [c], John J. Ramirez-Avila [d]

[a] Instituto Geofísico del Perú - IGP, Calle Badajoz #169, Mayorazgo IV Etapa, Ate Vitarte, Lima, Peru
[b] Programa de Maestría en Recursos Hídricos, Universidad Nacional Agraria La Molina, UNALM, Lima, Peru
[c] Institut des Géosciences de l'Environnement – IGE (Univ. Grenoble Alpes, IRD, CNRS, G-INP), 38000 Grenoble, France
[d] Watersheds and Water Quality Research Lab, Richard A. Rula School of Civil and Environmental Engineering, Mississippi State Univ., USA

ARTICLE INFO

Keywords:
Repiquetes
Riparian agriculture
Rainfall
Flooding risk
Western Amazon

ABSTRACT

Study region: The western Amazon basin at Tamshiyacu gauging station (near the Iquitos City) hosts floodplain agriculture that can be affected by the sudden reversal in direction of water levels known as "repiquetes" that produce intermittent flooding.
Study focus: This study assesses repiquete flooding risk in riparian crop areas based on statistical analyses of repiquete events registered from 1996 to 2018, hydraulic modeling to estimate flooded extension, and assessment of climatological characteristics during the formation of repiquetes.
New hydrological insights: Floods ($\geq$ 20 cm) produced by repiquetes in riparian crop areas between 83.00 and 88.00 m above sea level (masl) occur 1.8 times per year. However, not all elevation ranges have the same flooding risk to crops. Terrain elevations between 85.31 and 87.00 masl have a reduced flooding risk of 0.35 per year. Likewise, areas with elevations between 87.00 and 88.00 masl (43% of the total area) were not affected by repiquetes. Extreme repiquetes (study cases of 2002 and 2008) have been influenced by the increase of atmospheric moisture flux convergence and precipitation over both the northern Ucayali and Marañón basins through the six previous days. Flood impacts from the extreme event of 2002 (2008) could have reached 40% (25%) of the available area for agriculture at the initiation of the repiquete.

1. Introduction

The Amazon basin hosts biodiversity of aquatic and terrestrial plants and animals. These species have dynamic interactions due to the hydrological regime of their rivers, including variations in the flows and water levels between low-water and high-water periods (Sioli, 1984). The hydrological regimes of the Amazon rivers provide opportunities for agricultural activities. In the Amazon basin, communities have been established in high terrain elevations to prevent flooding and near the floodplains that have a great potential for agriculture (Coomes et al., 2016; Denevan, 1996; Gorenstein, 2023; Hiraoka, 1985; Jakovac et al., 2017; Jardim et al., 2020; WinklerPrins, 2022), due to these areas are enriched by nutrients from the Andes transported by rivers (Ronchail et al., 2018, 2016). The intensification of agriculture in the Amazon floodplain has increased due to population growth around cities and market demand

* Corresponding author at: Instituto Geofísico del Perú - IGP, Calle Badajoz #169, Mayorazgo IV Etapa, Ate Vitarte, Lima, Peru.
E-mail address: jonathan_valcar@outlook.com (J. Valenzuela).

https://doi.org/10.1016/j.ejrh.2023.101428
Received 6 November 2022; Received in revised form 14 May 2023; Accepted 17 May 2023
Available online 24 May 2023

for crops such as cassava and beans in Brazil, and rice in Peru (Chibnik, 1994; Coomes et al., 2016; Jakovac et al., 2017).

Nevertheless, agriculture along the floodplain is exposed to natural hazards, principally by river stage reversal or sudden floodings (repiquetes), as well as edaphic conditions that affect the economy of the riparian farmer families (List and Coomes, 2017). Repiquetes are events that can interfere with the cultivation of crops, i.e., they can remove and carry seeds downriver, shorten their vegetative period, flood agricultural areas, and destroy harvests. This study focused on analyzing flooding risks produced by repiquetes on floodplains used for agriculture in the Amazon basin.

In the western Amazon basin, agriculture is primarily developed on the floodplains and islands formed by the meandering river during the transition from the wet to the dry season. This occurs between June and October (Espinoza et al., 2011; Lavado-Casimiro et al., 2013). During that season, the water elevation drops by up to 7 m at the Tamshiyacu gauging station in the Amazon River, exposing the terrain available to recessional agriculture (Ronchail et al., 2018, 2016). In the lowland of the western Amazon basin, specifically in the Loreto department (49% of the western Amazon basin up to Peruvian Tamshiyacu station, Fig. 1a), rice is sown on average in 34,600 ha (2000–2010): 70% of which are floodplains (DIA, 2011; INIA, 2005). In the Ucayali province, this value is 6000 ha (Labarta et al., 2007).

Repiquetes are unpredictable and sudden reversals in the direction of river levels, both when the river level rises and falls (Coomes et al., 2016). However, for floodplains or recessional agriculture, repiquetes in the transition from wet to dry season are important and occur due to abundant rainfall episodes in the northern part of the western Amazon basin (Marañón basin). These episodes are associated with changes in the direction of the low-level meridional winds over the Andes-Amazon transition zone (Figueroa et al., 2020). Repiquete flooding can seriously affect crop productivity, thus compromising the economy and food security of many riverine communities.

A repiquete event on 28 June 2012 (06 July 2002) could have flooded 59% (88%) and 14% (52%) of the lateral silt bar used for recessional agriculture in the communities of Dos de Mayo and Augusto Freyre (near the City of Iquitos), respectively (List and Coomes, 2017). Recent work (List and Coomes, 2019) found that the mean potential production of rice in regions of the Peruvian Amazon along the Muyuy anabranching structure around the City of Iquitos decreased by 50% in 2012 due to both crop inundation and reduction of the growing time influenced by repiquetes. The occurrence of repiquetes has been estimated at 3.2 times per year (Coomes et al., 2016; Figueroa et al., 2020; Ronchail et al., 2018). However, not all repiquetes will flood agricultural areas, depending on the repiquete magnitude (risk magnitude of flooding), date of occurrence, and terrain elevation.

Previous studies have analyzed this phenomenon by considering hydrological or climatological approaches separately. However, the nature of the phenomenon suggests that both approaches should be used together, taking into account the climatological characteristics that allow the formation of these events, as well as the impacts on agricultural areas and the analysis of extreme events.

In order to investigate the repiquete phenomenon, two study questions were defined as follows: *Are repiquetes, which have the potential to cause flooding to agricultural areas, produced by precipitation over the north of the western studied Amazon basin, or is there another part of the basin influencing their occurrence? And Is it feasible to determine a secure zone for cultivation and assess flooding risk based on analyses of repiquetes?*

Answering these questions can support farmers in their decision-making process toward reducing or mitigating riparian crop loss in the western Amazon River basin. Thus, this paper reports a broad assessment of repiquetes that include: i) identifying repiquetes with risk magnitude of flooding and extreme events; ii) assessing the flooding risk by repiquetes based on terrain elevation of croplands and

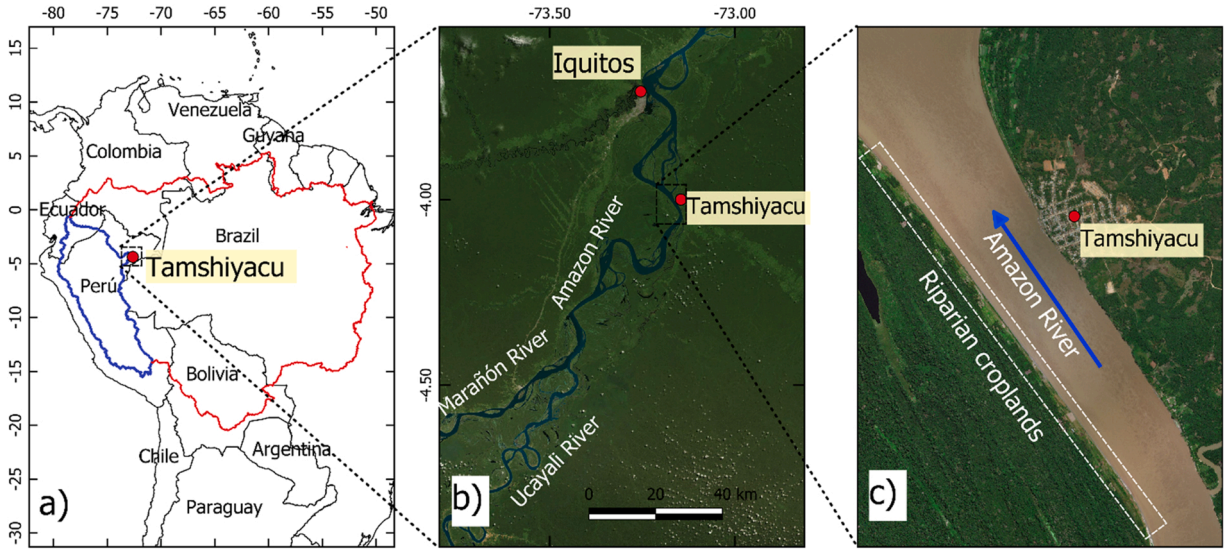

Fig. 1. a) The Amazon basin (red polygon) and the studied Amazon basin up to the Tamshiyacu gauging station located over the Peruvian and Ecuadorian Amazon (blue polygon); b) location of the Tamshiyacu gauging station on the Amazon River, the City of Iquitos, and the tributary rivers; c) location of the 4 km stretch on the Amazon River where the repiquete analysis was performed.

estimating the flooded areas as a function of the risk magnitude of repiquete; iii) characterizing the climatological behavior of repiquete formation that could be used to identify future events; and iv) assessing the probable flooding impact produced by extreme repiquete events. A combined approach was used to answer the study questions and objectives. The approach includes statistical analyses of repiquetes, remote sensing detailed topography survey, hydraulic modeling, and climatological assessment. The results could help develop risk maps to guarantee floodplain agriculture, which could be handed to regional authorities.

2. Data and methods

2.1. Study area and atmospheric and hydrology features

The Amazon River is the largest fluvial system in the world in terms of the volume of water exported to the ocean (209,000 m^3/s), its drainage area of 6.2×10^6 km^2 (Callède et al., 2010), and its suspended sediment export (1200 Mt/yr) (Armijos et al., 2020). It is the backbone of the natural Amazon ecosystem, with high biodiversity in flora and fauna (Foley et al., 2007). The principal sources of food and economic revenue for human settlements established along the river margins are agriculture (rice, manioc, peanuts) and fishing (Gorenstein, 2023; Jakovac et al., 2017; Labarta et al., 2007; List and Coomes, 2017).

The Amazon basin drains into the Tamshiyacu gauging station at the mainstream Amazon River, which is downstream of the confluence of the Marañón and Ucayali Rivers (Figs. 1a, 1b). It covers an area of approximately 750,000 km^2 in the Peruvian and Ecuadorian Amazon (Armijos et al., 2013) in the western Amazon basin region. Around Tamshiyacu City, the flooding risk zone has an extension of 4 km along the left bank of the Amazon River (Fig. 1c).

The spatiotemporal rainfall variability in the western Amazon basin is associated with the meridional extension of the region, its tropical location, and the complex topography delineated by the transition between the Andean highlands and the western forest. These can all influence the atmospheric dynamics and thermodynamics of the region (Costa et al., 2021; Figueroa and Nobre, 1990). The rainy season occurs during the austral summer (December–February) along the southern region; this rainfall is related to the late phase of the South American Monsoon System (SAMS) and regional features such as the Bolivian high and the South American low-level jet (LLJ) (Espinoza et al., 2020; Marengo et al., 2004; Satyamurty et al., 1998; Vera et al., 2006). The northern region practically lacks a dry season (June–August), and bimodalities are registered in the annual cycle influenced by the Intertropical Convergence Zone (ITCZ) and the climatological westward moisture transport (Laraque et al., 2007; Segura et al., 2019). A strong gradient of precipitation depth – conditioned by the topography and exposure to easterly winds – has been documented over the Andes-Amazon transition zone ranging from 250 to 6000 mm/yr. In the southern region, peaks of precipitation called rainfall hotspots regions are found around the 1000 masl and are related to LLJ, the dynamics, and thermodynamics of local features driven by the orography and thermal heating (Chavez and Takahashi, 2017; Espinoza et al., 2015; Junquas et al., 2018). The northwest equatorial region is also one of the rainiest zones, with over 3000 mm/yr (Espinoza et al., 2009).

Regarding rainfall dynamics in the region, an organized evolution of northerly to southerly regimes of atmospheric circulation phases, also named circulation patterns, are related to the northward propagation of rainfall (Espinoza et al., 2021, 2012; Paccini et al., 2018). These changes in circulation are associated with alternating (negative to positive) geopotential anomalies over the South American continent and surrounding oceans. These anomalies are driven by the intrusion of extratropical systems into subtropical and tropical areas. This process destabilizes the atmosphere along their path. At intra-seasonal time scales (mainly 30–90 days), this region is also influenced by the eastward propagation of the Madden-Julian Oscillation (MJO) as described in previous studies (Mayta et al., 2019; Recalde-Coronel et al., 2020).

Other studies in the western Amazon basin have established relationships between convection activity, rainfalls, and the meridional and zonal regimes. For example, the southerly cross-equatorial regimes have been found to enhance convection and precipitation over the northern Amazon (Jones and Carvalho, 2002; Wang and Fu, 2002).

The rainfall variability in the western Amazon produces high river flow discharges at the Tamshiyacu station from April to June and low flow discharges from August to October, with a mean discharge of 32,000 m^3/s (Espinoza et al., 2013, 2009). Peak flows are usually observed at the beginning of May, and the lowest discharges are observed in mid-September (Ronchail et al., 2018). The minimum and maximum mean levels (discharges) at the study station, from 1985 to 2019, are 81.42 masl (12,600 m^3/s) and 89.72 masl (46,300 m^3/s), respectively. The highest and lowest historical levels (discharge) observed at this station were, respectively, 91.32 masl (55,400 m^3/s) on 19 April 2012 (Espinoza et al., 2013) and 79.64 masl (8300 m^3/s) on 05 September 2010 (Espinoza et al., 2011).

The channel of the Amazon River along the segment between the Tamshiyacu and Iquitos gauging stations (Fig. 1) is made of fine sands with a median particle size (d_{50}) of around 0.3 mm (Mendoza et al., 2016). The channel has an average water slope of 0.00004 m/m.

2.2. Dataset description

The daily discharges and water level time series used in this study were obtained from the SO-Hybam database from 01 January 1996–31 December 2018. These datasets are available at: <https://hybam.obs-mip.fr/es/website-under-development-3/> .

Daily precipitation was obtained from Climate Hazards Group InfraRed Precipitation with Station (CHIRPS) using a spatial resolution of 0.25° from 01 January 1996–31 December 2018, available at: <https://data.chc.ucsb.edu/products/CHIRPS-2.0/> . CHIRPS dataset was selected for this study instead of another source of datasets due to its better performance when retrospectively evaluating extreme hydrological events in the Amazon basin (Wongchuig-Correa et al., 2017). In addition, the analysis of precipitation

datasets, which combine both reanalysis data, satellite estimates and in situ observations, together with circulations and meteorological variables throughout the troposphere, is a common practice (González-Rojí et al., 2022; Paccini et al., 2018).

Atmospheric data were analyzed using winds and specific humidity at 1000–300 hPa from the European Centre for Medium-Range Weather Forecasts reanalysis ERA-Interim (Dee et al., 2011) with a spatial resolution of 0.25° over the study region.

The vertical system of reference used here is the benchmark network developed by SO-Hybam based on the Earth Gravitational Model of 2008 (EGM08).

To determine the extent of the riparian agricultural zone and the flooding risk to crops, a Digital Elevation Model (DEM) of 1 m (spatial resolution) was generated for the area of interest. It was composed by adding the photogrammetric topography of the left bank developed using a remotely piloted aircraft system (RPAS) with real-time kinematic positioning, a bathymetry (surveying of the channel bottom using a single-beam echosounder by sending an acoustic signal) with cross-section separation of 250 m, and the digitizing of the 10 m spatial resolution Sentinel 2 satellite imagery for the right bank. Twelve ground control points were positioned for the RPAS flight. These were performed 60 m above the ground considering an 80% longitudinal and transversal overlap. The ground sampling distance was 1.64 cm per pixel. A total of 1325 photographs were taken, generating a cloud of 967 million points to represent the terrain surface. The mean vertical error of the photogrammetric DEM was 5 cm.

2.3. Repiquete characterization

A repiquete has been defined as a reversal in the water level of rivers greater than 1 cm (Coomes et al., 2016). This study focused on repiquete events that occur during the transition from the wet to dry season and when the water level increase is equal to or greater than 20 cm because these changes could represent a crop risk. The peak elevation of a repiquete is the highest elevation of the water level observed during an event. For agriculture along the riparian zone of the Amazon River, the peak elevation could be harmful if it reaches the elevations being used for crops. The magnitude of a repiquete is defined by the difference between its peak and initial water elevation. The risk magnitude of each repiquete was defined as the portion of the magnitude equal to or greater than 20 cm developed in the agricultural elevations.

The 73 repiquetes equal to or greater than 20 cm reported by Figueroa et al. (2020) between 01 January 1996 and 31 December 2018 (Table S1) were used here to identify the repiquetes with risk magnitude along the riparian zone of the Amazon River at Tamshiyacu City. After identifying the repiquetes and their peak elevations, the area available for crop production and the frequency of occurrence of the repiquetes associated with percentiles of peak elevations were used to define the flooding risk for elevation ranges. Percentiles from the 70th to the 100th were considered to guarantee the major available area for crop production and the least flooding risk.

Extreme repiquete events have been identified considering the mean risk magnitudes plus one standard deviation. Two extreme events have been selected as case studies based on their risk magnitude and duration. The first event is the highest repiquete in terms of risk magnitude. The second is a repiquete representing the remaining extreme repiquetes regarding risk magnitude.

2.4. Climatologic assessment of repiquetes

To look for atmospheric conditions related to the beginning of repiquetes with a potential for flooding crops, a composite of integrated vertical humidity flux and precipitation anomalies was computed at each grid point by subtracting the first harmonics from the 1981–2010 period. This step used daily horizontal components of wind and specific humidity at 1000–300 hPa from the Era-interim reanalysis (0.25°, Dee et al., 2011). Daily precipitation registers from the Climate Hazards Group InfraRed Precipitation with Station (CHIRPS) v.2 (0.25°, Funk et al., 2015) were also analyzed. Furthermore, mean daily precipitation and its distribution over the region were computed for each repiquete selected. These were initiated and raised above the minimum elevation farmers have used for rice cultivation along the riparian zone of the Amazon River. Similar analyses were used to assess extreme repiquetes events.

2.5. Repiquete simulation

The US Army Corps of Engineers (USACE) Hydrologic Engineering Center – River Analysis System (HEC-RAS) 1D model v6.1 was used to simulate the possible flooding caused by the studied repiquete to obtain the flooding boundary caused by the repiquete peak in agricultural areas. The HEC-RAS 1D model was selected following a comparison with its 2D counterpart for the analyzed straight reach of the Amazon River. The performance of the HEC-RAS 1D model in estimating the extent of flooded areas was found to be similar to that of the HEC-RAS 2D model.

Determining the flooding boundary is necessary to estimate the impact of the repiquetes on crops by assessing the percentage of the area flooded by the repiquete versus the available area at the beginning of the repiquete. Peak elevations associated with each percentile were simulated under steady flow conditions along a 4 km stretch of the Amazon River at the Tamshiyacu gauging station. Similarly, an unsteady flow simulation was performed to represent the hydrograph of the two extreme repiquetes previously identified. To establish the model, 74 cross-sections were extracted from the DEM, considering a cross-section spacing of 50 m. The initial manning roughness coefficient was determined based on the composition of the river bottom and banks. Flow discharges and elevations were determined using the rating curve of the Tamshiyacu gauging station, which has been used as the downstream boundary condition of the model.

3. Results

3.1. Available areas and repiquetes events

From the photogrammetric survey, the elevations of the riparian zone used by farmers to plant rice crops along the study area were estimated and ranged from 83 to 88 masl. The area has an average width of 50 m and an extent of about 180,000 m^2. The average topographic gradient of the area used for rice cultivation is 0.1 m/m.

The relationship between the percentage of available area for rice crops and the land elevation for the recession period is shown in Fig. 2. The available area for rice cultivation increases as the water level drops. If the water level drops from 88 to 87 masl (only 1 m), then 43% of the total available area is exposed due to its small topographic gradient (0.05 m/m). However, the water level needs to drop 4 m (87–83 masl) to expose the remaining 57% of the total available area.

An average rate of 3.2 repiquetes per year was estimated from 01 January 1996–31 December 2018. Of the 73 repiquetes, only 42 (with a ratio of 1.8 repiquetes per year) had a risk magnitude (orange bars equal to or greater than 20 cm in Fig. 3) and could potentially flood crops based on the impact of their magnitude in the agricultural zone (83–88 masl). Repiquetes 53 and 65 (circled in red in Fig. 3) have not been considered in the analysis because they occurred before the rice crop planting dates and did not imply impacts on agriculture.

The mean risk magnitude of the 42 repiquetes was 0.68 m with a standard deviation of 0.47. Considering intervals of risk magnitudes of 20 cm for the total 42 repiquetes, 31.2% (13 repiquetes) have a risk magnitude between 0.20 and 0.40 m, 28.8% (12 repiquetes) between 0.40 and 0.60 m and the remaining 40.0% (17 repiquetes) are distributed between 0.6 m y 2.4 m. Additionally, 41 repiquetes have a risk magnitude of less than 1.4 m, and only one repiquete has a risk magnitude of 2.34 m (repiquete of the 2002 year) (Fig. 4). Extreme values of risk magnitude of the repiquetes have been identified by referencing the mean plus one standard deviation (1.15 m). Repiquetes observed in the years 1998 (1.28 m - No. 7), 2000 (1.4 m - No. 12), 2002 (2.34 m - No. 16), 2008 (1.29 m - No. 36), 2010 (1.35 m - No. 43), and 2018 (1.22 m - No. 72) have been identified as repiquetes with extreme risk magnitude (Fig. 3).

3.2. Flooding risk areas

Fig. 5a shows the relationship between the risk magnitude of the 42 repiquetes with the potential risk of flooding croplands and the flooded area of the cropland. The fitted linear relationship indicates that a mean cropland area of approximately 13,829 m^2 is flooded by a repiquete with a mean risk magnitude of 0.68 m, representing 8% of the total cultivation area. A repiquete with a risk magnitude of 1.41 m would flood an average of 32,360 m^2 of cropland, representing 18% of the total agricultural area available along the riparian zone.

We next compared the flooded area estimated by the hydraulic simulation (62,796 m^2) with the predicted flooded area for the highest risk magnitude event that occurred on 06 July 2002: The linear relationship underestimates this value by around 6824 m^2 (10% of the flooded area). Certainly, the flooded area depends on the topographic gradient of the elevation range where the repiquete is developing. The percentage of the area flooded by a repiquete (to evaluate the flooding impact) depends on the available area at the initiation of the repiquete (Fig. 2).

The flooding risk area is related to the percentiles of the peak elevation for the 42 repiquetes with risk magnitudes that potentially flood croplands, the area available for crops, and the frequency of the repiquetes (Fig. 5b). A negative correlation (r^2 =0.97) between the percentile of peak elevations and the frequency of repiquetes indicates that higher values of percentiles result in lower values of frequency of the repiquetes, thus referencing a low flooding risk of the riparian zone area above the elevation associated with that percentile. Similarly, a negative correlation (r^2 =0.99) exists between the peak elevation and the area available for rice cultivation over

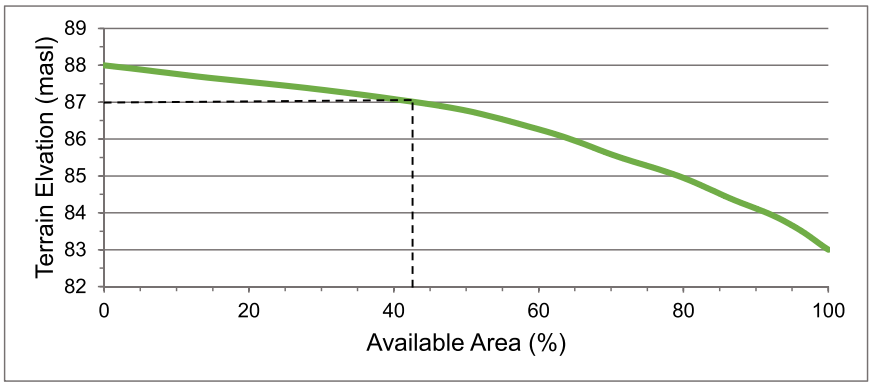

Fig. 2. Relationship between the available area (in percentage) to use for agriculture and the land elevation of the riparian zones in front of Tamshiyacu City in the green line. The total area used for agriculture is located between 83 and 88 masl, and 43% of the total available area is located between 87 and 88 masl as shown in black dotted lines.

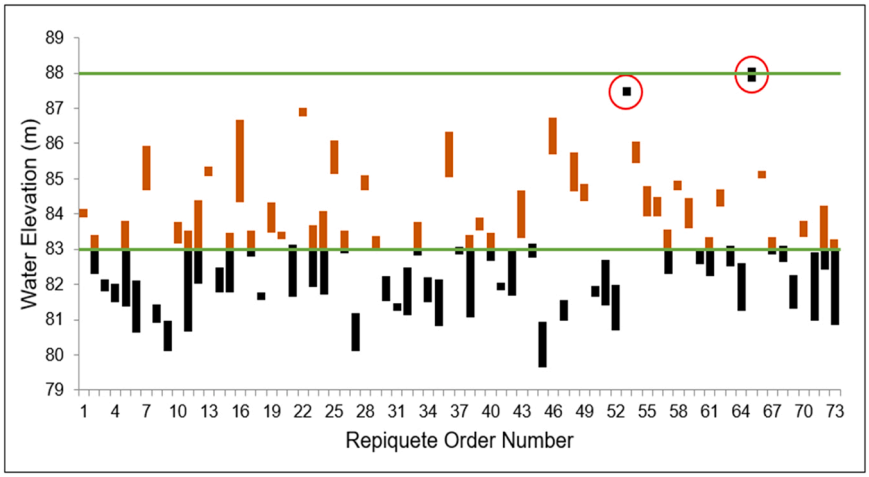

Fig. 3. Repiquetes observed at the Tamshiyacu gauging station ordered by date of occurrence from 1996 to 2018 versus their magnitude considering the minimum elevation of the repiquete (first day) and the peak elevation. The risk magnitude of 42 repiquetes is represented by orange bars. The repiquetes enclosed by the red circle were not analyzed. The green lines show the elevations where agriculture is developed (83 masl – 88 masl).

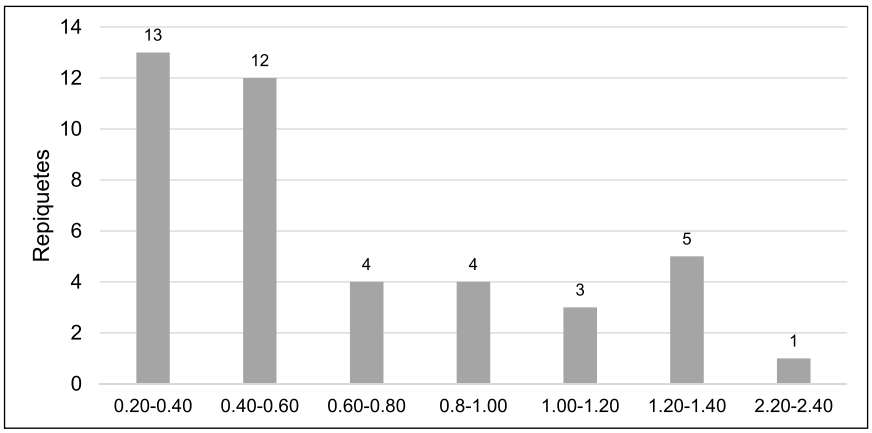

Fig. 4. Total number of repiquetes with associated risk magnitude distributed in intervals of 20 cm.

the percentile. The area available for rice cultivation related to crop productivity is smaller for higher percentiles of peak elevation (Table 1).

The assessment of the flooding risk associated with the frequency of occurrence of repiquetes (with risk magnitude) shows that the frequency of occurrence of repiquete events that could affect crops is 0.35 repiquetes per year (i.e., one time per 3 years) for terrain elevations above 85.31 masl (80th percentile of peak elevations). However, the area below 85.31 masl has a flooding risk of 1.47 repiquetes per year (i.e., three times per 2 years). Similarly, for terrain elevations above 85.91 masl (90th percentile of peak elevations), the flooding risk associated with the frequency of occurrence is reduced to 0.26 repiquetes per year. Terrain elevations over the 87.01 masl do not present flooding risk per occurrence of repiquetes, and, as mentioned before, these elevations represent 43% of the total available area for agriculture. The flooding boundary corresponding to the 80th and 85th percentiles obtained by hydraulic modeling is shown in Fig. 5c.

3.3. Formation of repiquetes with risk magnitude

To describe the formation of repiquetes with risk magnitude that potentially flood croplands at the study site, a composite of vertically integrated moisture flux and precipitation anomalies was computed from the 42 events with risk magnitude that affected the area used to grow rice. Based on the day of a repiquete initiation at the Tamshiyacu gauging station (d0), high values of moisture convergence were found between the sixth and the third preceding days (d-6 and d-3) to the north of 7°S. This convergence was driven by the increase in an easterly moisture flux anomaly of 55 kg/m/s (Fig. 6). The same days registered the maximum precipitation anomalies over the northwest sub-basins of the Marañón basin.

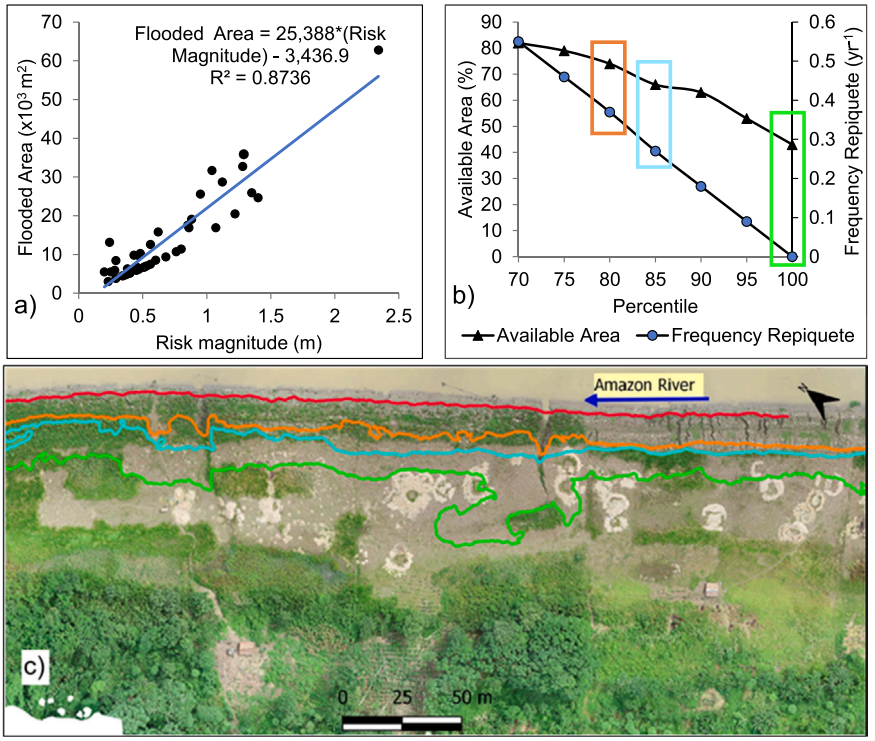

Fig. 5. a) Linear relationship between the risk magnitude of repiquetes and the flooded area by the repiquete; b) relationship between the percentile of the peak elevation and the available cropland area percentage (black triangles) as well as the percentile of the peak elevation and the repiquete frequency (blue circles); c) a portion of the study area where it is possible to observe the rice crops already cultivated within the limits of the area where the repiquetes impact agriculture (between the red and the green lines). The elevation corresponds to 83.00 masl (red line), the 80th percentile of 85.31 masl (orange line), the 85th percentile of 85.91 masl (cyan line), and 87.01 masl (green line) to the 100th percentile. The blue arrow indicates the direction of flow.

Table 1
Peak elevation, number of repiquetes that exceed the peak (n), percentage of available area on the riparian zone for crop production, and the number of repiquetes per year (frequency) estimated for each percentile of the total number of repiquetes that potentially flood cropland. The frequency (repiquetes per year) shows the number of repiquetes divided by the range of years analyzed (n/23).

Percentile	Peak elevation (masl)	Number of repiquetes that exceed the peak (n)	Available Area (%)	Frequency (repiquetes/year)
70	84.83	13	82	0.57
75	85.05	11	79	0.48
80	85.31	8	74	0.35
85	85.91	6	66	0.26
90	86.09	4	63	0.17
95	86.64	2	53	0.09
100	87.01	0	43	0.00

3.4. Evaluation of repiquetes with an extreme magnitude of risk

Two cases of the six repiquetes were identified with extreme flooding risk. The selection was based on the high-risk magnitude and long duration of repiquetes that potentially generate impacts on agricultural production in the region. The repiquete observed on 06 July 2002 has the highest risk magnitude (2.34 m) in the analyzed period (1996–2018). The repiquete observed on 17 June 2008 has a magnitude (1.29 m) similar to the mean of the remaining five extreme repiquetes with a high-risk magnitude (mean risk magnitude = 1.31 m). The repiquetes of 06 July 2002 and 17 June 2008 are shown in Table 2 and Fig. 7a. Flooded areas for the 2002 (purple) and 2008 (oranges) repiquetes are shown in Figs. 7b and 7c, respectively. The flooded areas were determined based on the non-steady hydraulic simulation considering the hydrographs shown in Fig. 7a.

The 2002 extreme repiquete event had a risk magnitude of 2.34 m, an average inundation width of 15 m, and a duration of 42 days (Fig. 7b). The flooded area caused by this repiquete was estimated at 62,796 m^2 representing 40% of the area available for agriculture at the initiation of the repiquete (157,000 m^2). This repiquete event was initiated with a heavy precipitation intensity over the

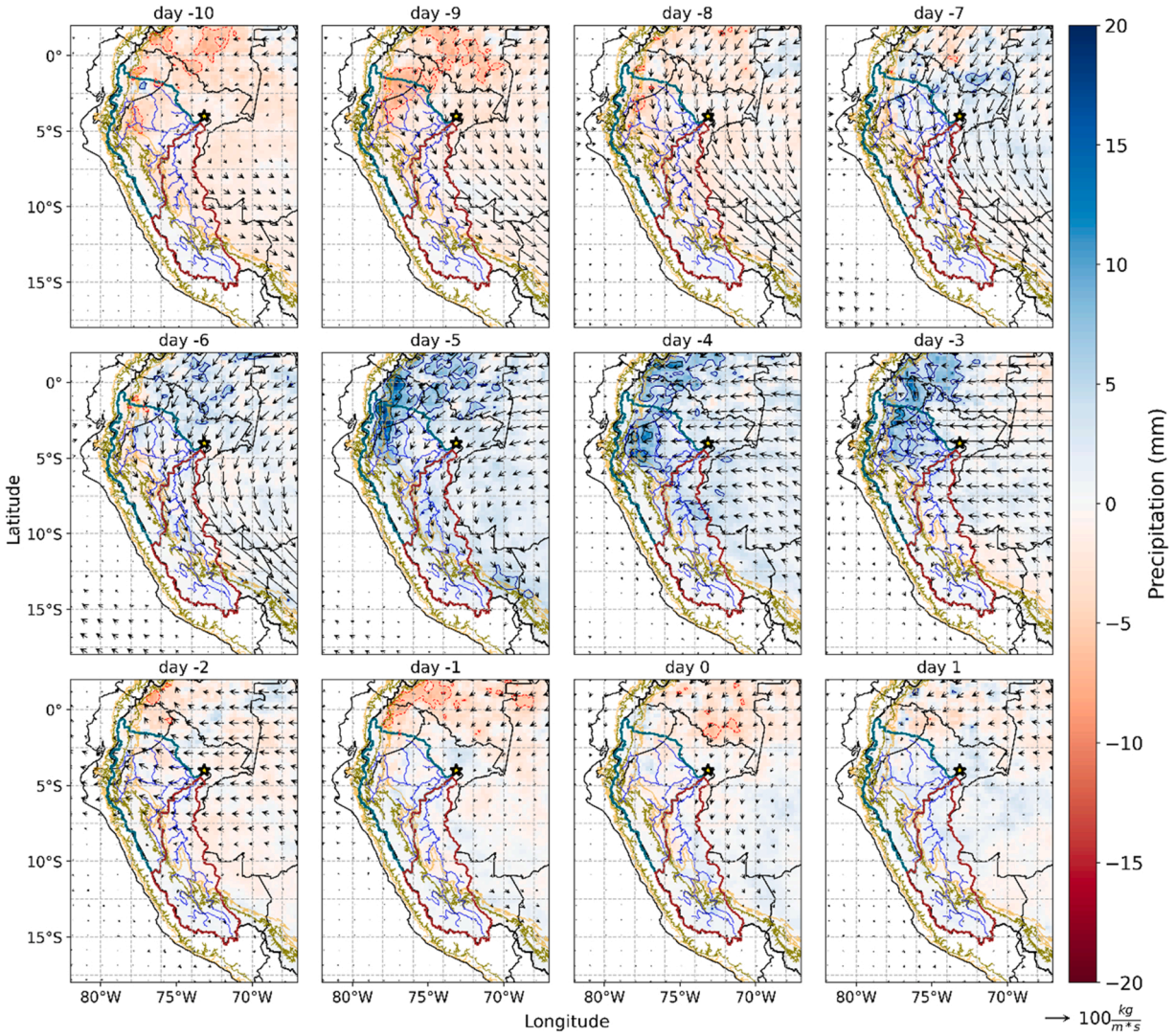

Fig. 6. Composite of vertically integrated moisture flux (ERA-Interim, 0.25°) and daily rainfall anomalies (CHIRPS, 0.25°) from the preceding ten days (d-10) to the first day after (d+1) of the 42 high magnitudes repiquetes that affected the area used by farmers to plant rice crops at the Tamshiyacu gauging station (star). Marañón (Ucayali) River basin are delineated in cyan (red). River networks are delineated in blue. Yellow and dark yellow lines represent elevations of 500 masl and 1500 masl, respectively.

Table 2
Information about the repiquetes of July 2002 and June 2008, dates, elevations, and risk magnitude and duration of the event.

Year	Initiation date	Peak date	Finish date	Start Elevation (masl)	Peak Elevation (masl)	Risk Magnitude (m)	Duration (days)
2002	07/06/2002	07/24/2002	08/17/2002	84.32	86.66	2.34	42
2008	06/17/2008	07/02/2008	07/10/2008	85.03	86.32	1.29	23

northern Marañón (Pastaza sub-basin) and northern Ucayali basins on 01 July (d-5) and was reflected at the Tamshiyacu gauging station on 06 July (d0). The magnitude of the repiquete increased via the precipitation over the Marañón basin from 02 July (d-4) to 16 July (d+10). Precipitation exceeded the 90th percentile of the JJA (June-August) period in the northern Marañón basin, predominantly over the Pastaza and Tigre sub-basins, on 17 July (d+11) and 18 July (d+12). These precipitation events led to a peak of the repiquete observed at the Tamshiyacu gauging station between 23 July (d+17) and 24 July (d+18). Precipitation over the northern Marañón basin (Pastaza, Morona, Santiago, and Nieva sub-basins) exceeded the 90th and 99th percentiles on July 23rd and 24th, respectively. These precipitation events and the one that occurred on 26 July (d+20) kept the magnitude of the peak of the repiquete relatively stable for almost 2 weeks (Fig. S1).

During the days that preceded the dates of the studied repiquete, the easterly vertically integrated moisture flux was higher than

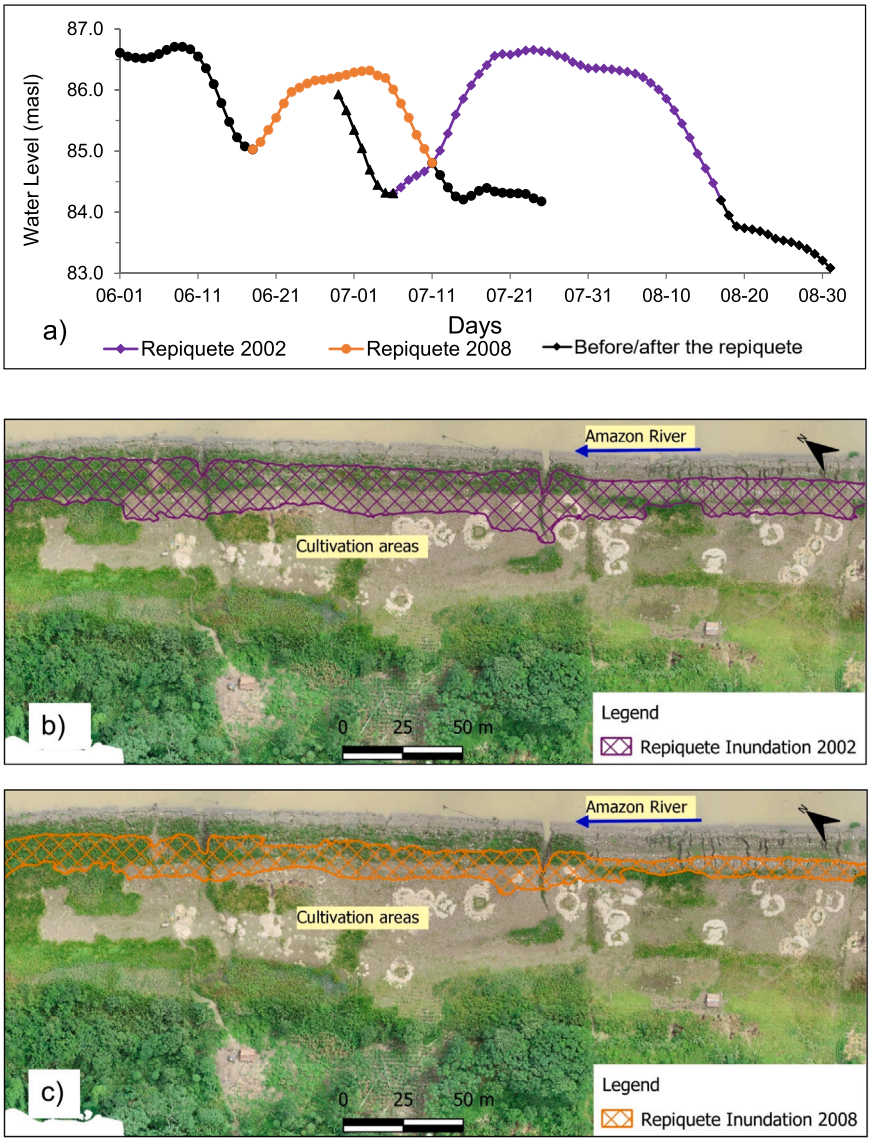

Fig. 7. a) Hydrographs of the 2.34 m (2002) and 1.29 m (2008) repiquetes including water levels before and after the event; b) flooded area over the terrain used to plant rice crops by the 2002 repiquete (crops already cultivated shows in the figure); c) area flooded by the 2008 repiquete. The blue arrow in b) and c) indicates the direction of flow.

250 kg/m/s, and the convergence to the west of 74°W was intense over the northern area of the basin. After the repiquete, the flux was 200 kg/m/s.

The contribution of the Marañón's sub-basins is greater than the Ucayali sub-basins when considering both the mean areal daily and the accumulated precipitacion, for the days before the event (Fig. 8a and c). At the beginning of the event, the northern watersheds registered the maximum accumulation of rainfall, although watersheds below 1500 masl within the Ucayali basin also contributed. In addition, a major contribution by the northern watersheds was noticed during the 2002 event (Fig. 8d).

On the other hand, the 2008 extreme repiquete had a risk magnitude of 1.29 m (d+16) and lasted 23 days. The area flooded by this repiquete was estimated to be 35,800 m^2, or a quarter of the area available for cropping along the riparian zone at that time (142,000 m^2). The average inundation width was 9 m (Fig. 7c), and its origin was related to both the main tributary basins of the Peruvian Amazon River.

The event of 2008 was initiated on 17 June (d0) at the Tamshiyacu station due to a combination of precipitation over the northern Ucayali basin on 10 June (d-7) as well as values over the northern low Marañón basin in subsequent days. From 11 June (d-6) to the 21 June (d+4), the precipitation over the Ucayali and Marañón basin increased the water elevation at the Tamshiyacu gauging station. The accumulated precipitation in June exceeded the 95th percentile of the JJA period over the Marañón (Tigre, Pastaza, Morona, Santa, and Nieva sub-basins) and the northwest Ucayali sub-basins on 22 June (d+5) and 24 June (d+7), respectively (Fig. 8b). The

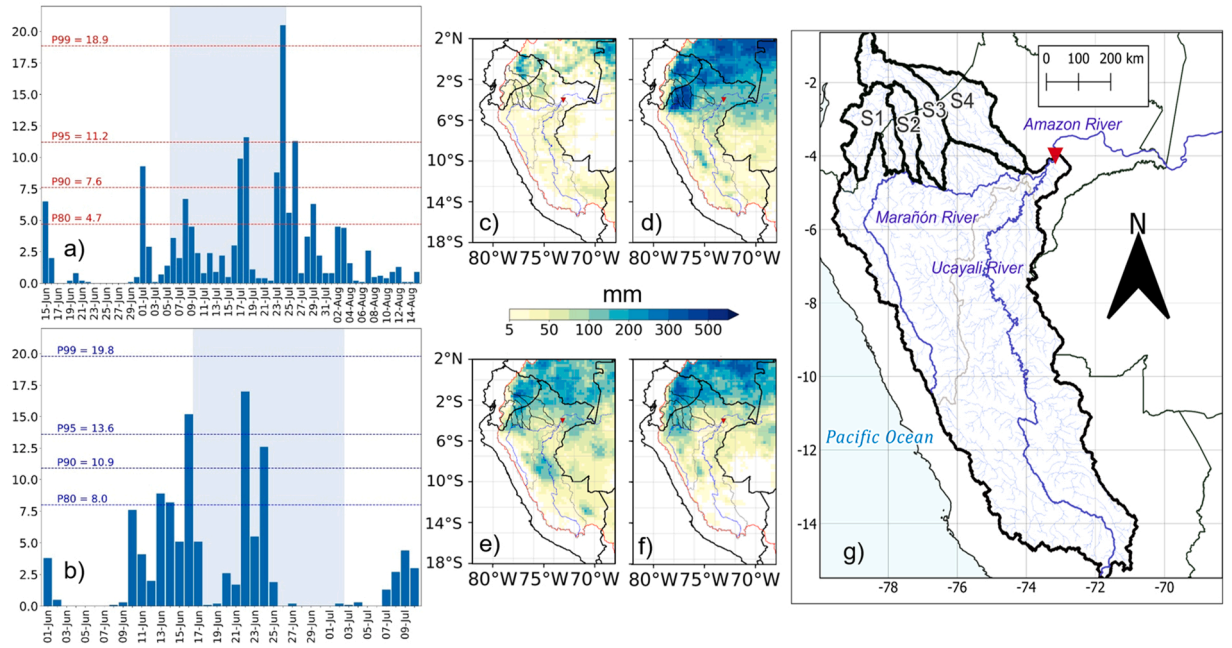

Fig. 8. a) Mean areal daily precipitation (mm) over the western Amazon basin at the Tamshiyacu station for the 2002 repiquete from 15 June to 15 August with d0 on 06 July; b) mean areal daily precipitation (mm) over the western Amazon basin at the Tamshiyacu station for the 2008 repiquete from June 1st to July 10th, with d0 on June 17th. The percentiles concerning the JJA (annual) period are plotted in red (blue) lines, and the light blue shaded area represents the period between the date of initiation and peak of repiquete; c) accumulated precipitation (mm) from d-10 to d0 for 2002 repiquete; d) accumulated precipitation from d0 up to the peak date of 2002 repiquete; e) accumulated precipitation (mm) from d-10 to d0 for 2008 repiquete; f) accumulated precipitation from d0 up to the peak date of 2008 repiquete. The sub-basins of the northern Marañón basin are shown in black polygons in panels c, d, e, and f; g) from left to right, the Santiago (S1), Morona (S2), Pastaza (S3), and Tigre (S4) sub-basins of the northern Marañón basin are shown, and the Tamshiyacu station indicated by a red triangle.

peak of the repiquete at the Tamshiyacu gauging station was observed on 02 July (d+15) (Fig. S2). These days are consistent with the moisture convergence observed to the west of 72°W along the watershed. The easterly vertically integrated moisture flux with values higher than 200 (250) kg/m/s was identified in d-6 (d-1 and d+7).

The peak of the 2008 repiquete could be related to a later dynamic wave due to a major precipitation contribution of the western watersheds (Fig. 8e and f) or an influence of lateral humid zones that drain into the riverbed.

4. Discussions

The analyses of this study are based on remote sensing, field measurements, hydraulic simulations, and climatological assessments. They provide new insights into how repiquetes impact riparian croplands in the recession period of the western Amazon basin. Here, 42 of the 73 repiquetes (1996–2018) identified by Figueroa et al. (2020) with risk magnitudes up to 2.34 m had the potential to flood riparian agriculture. Here, 41 of these repiquetes have a risk magnitude smaller than 1.41 m, and only one exception exceeds this risk magnitude. Our results focused on the 42 repiquetes that complement previous studies on this region (Coomes et al., 2016; Figueroa et al., 2020; List and Coomes, 2017; Ronchail et al., 2018). This prior work determined the flooding risk of riparian croplands based on terrain elevation, the characterization of climatological behavior of repiquete formation, and the likelihood of probable flooding impact produced by extreme repiquete events.

Rice crops in the lower Amazon region of Peru (departments of Loreto and Ucayali) cover an area of 25,000 ha of silt and sand bars (DIA, 2011; INIA, 2005). Thus, to avoid the 40% losses by farmers related to flooding in these areas, the National Institute of Agrarian Innovation (INIA, 2007, 2005) has developed the “Ecoarroz” and “JAR-I” – special rice varieties for the lowlands of the Amazon basin whose main characteristic is the reduction of the vegetative period (102–105 days) with a high yield (5–6 tons/ha). Surveys carried out with farmers in Tamshiyacu City (n = 29) reported that 52% of them used seeds of the variety “Esperanza”, and 38% were of the variety “Capirona” developed for highland regions of the Amazon basin. These varieties were adapted to Amazon highland soils and are resistant to pests. They have a high vegetative period of 120 and 150 days and potential yields between 9 and 11 tons/ha; however, the productivity decreases to 2.6–4.8 tons/ha in low-lying areas due to the difference in climates and soils condition (INIA, 2010, 2001; List and Coomes, 2019).

Importantly, there are currently no government programs that provide technical assistance to farmers on seed variety selection. This likely explains why this community does not use the variety and certified seeds adapted to the flooding, and only 30% of farmers know about the events of repiquetes. Therefore, selected varieties of rice seeds could be used by farmers based on a range of terrain

elevations as well as the frequency of occurrence of repiquetes to reduce crop losses and obtain better productivity. In this study area, 43% of the riparian area available for crop establishment (83–88 masl) is located between 87 and 88 masl and is considered a secure zone for cultivation because it would not be affected by repiquetes. Due to the low terrain gradient, this riparian area could be exposed in about 2 weeks, considering that the water level falls at 7.4 cm/day as determined for elevations of 84.75–87.55 masl (Ronchail et al., 2018). Farmers could use this 43% area for seeding the high vegetative period as Capirona variety. This strategy can lead to better productivity in terms of potential yield (tons/ha). The flooding risk by repiquetes is present in the remaining 57% of the available area.

Flooding risk by repiquetes increases when the elevation decreases. For terrain elevations between 85.31 and 87.00 masl (80th percentile of peak elevations of repiquetes), the repiquete rate is once every 3 years. It is better to use short vegetative period seeds of rice variety as JAR-I in this area. Similarly, Coomes et al. (2016) studied the Muyuy and Panguana anabranching structures (10 km on average downstream of Tamshiyacu City) on terrain elevations between 112 and 116 m of relative vertical datum (equivalent to 82.77–86.77 masl based on EGM08). These areas were used as cultivation rice areas, and they found a lower probability of flooding by the repiquete for elevations above 114 m (84.77 masl). The elevations farmers use in Muyuy anabranching are lower than those determined in Tamshiyacu City (decreasing from upstream to downstream). This implies that farmers consider the hydraulic gradient of the Amazon River to select agricultural areas. Consequently, the flooding risk by repiquetes based on percentiles could be extrapolated through 30 km downstream (before the Iquitos gauging station) and 30 km upstream. There is no important tributary in this area. For this extrapolation, one must consider the hydraulic gradient of the Amazon River at this reach of 0.00004 m/m. For example, 85.31 masl (80th percentile) at the Tamshiyacu gauging station would be 84.11 masl 30 km downstream due to the decrease in water level at this hydraulic gradient. To extrapolate to a large reach (i.e., Tabatinga gauging station in Brazil, at 508 km downstream of Tamshiyacu gauging station), one must use intermediate gauging stations and evaluate the tributaries in the reach (e.g., Napo River, Ampiyacu River, Atacuari River, Loretoyacu River). Similarly, one must use a hydrological distributed model for large basins such as the MGB model, i.e., evaluating the wave propagation of the hydrograph over a large scale (between Tamshiyacu and Tabatinga gauging stations) representing repiquetes events (Collischonn et al., 2007; Pontes et al., 2017; Wongchuig-Correa et al., 2017; Zubieta et al., 2015).

Risk magnitudes of repiquetes smaller than 0.60 m are common in the study area (25 of 42 repiquetes). The linear regression between the risk magnitude and the flooded area identified here indicates that the agricultural areas flooded by repiquetes with risk magnitudes of 0.40 m and 0.60 m are 4% and 7%, respectively, of the total available area. The occurrence of several independent repiquetes events with a small risk magnitude in a single year can be as significant as an extreme repiquete event. For instance, in 2013, four independent repiquetes events with risk magnitude were identified. The total sum of the magnitudes of each repiquetes event that occurred on 16 July (0.62 m), 22 August (0.88 m), 04 September (0.56 m), and 26 September (0.56 m) 2013 was 2.62 m, which exceeded, in terms of magnitude, the highest extreme repiquete event of 2.34 m. The sum of the percentages of the flooded area by each repiquete could rise to 35% of the total available area. However, to estimate the actual crop losses by the occurrence of repiquetes, one must analyze these events individually, considering the available area at initiating the repiquete.

The formation of repiquetes with the risk magnitude analyzed here is associated with high moisture transport and precipitation values over the northwestern Andes-Amazon sub-basins of the Marañón basin until 6 days before the initiation of the repiquetes. These results agree with Figueroa et al. (2020) and Ronchail et al. (2018). During the days that preceded the dates of the studied repiquete, the easterly vertically integrated moisture flux was higher than 250 (200) kg/m/s, and the convergence to the west of 74°W was intense over the northern area of the basin. After the repiquete, the flux was 200 kg/m/s.

Northeasterly and southeasterly fluxes are predominant climatological characteristics for the lower and mid-levels of the study region during JJA (Poveda et al., 2014; Trachte, 2018). Anomalies of the moisture flux convergence are around 50 kg/m/s during these days, which could increase the equivalent potential temperature at low levels and eventually trigger convection (Wright et al., 2017). Generally, the Mesoscale Convective Systems (MCSs) formed in the Andes-Amazon transition regions of Peru and Ecuador (Campozano et al., 2018) migrate towards the lowland forest, and those that form between the northern area of Peru, Brazil, and Colombia migrate to the west or southwest during JJA (Rehbein et al., 2018).

Versus the 2008 repiquete, the high magnitude and duration of the 2002 repiquete were probably induced by the higher precipitation distributed over the region that held over in the northern Marañón basin. However, these case studies of repiquetes with extreme risk magnitudes show the importance of the northern Ucayali basin, where a regional precipitation hotspot is located between 8° and 9.5°S and to the east of 74°W (Fig. 8). This part of the basin also influences the initiation and the peak of the repiquetes with extreme risk magnitudes. This finding is particularly important considering the nature of precipitation during extreme repiquetes, including large convective zones over the Peruvian Amazon lowland and orographic forced precipitation, as documented by Figueroa et al. (2020). What modulates the high precipitation events that occur successively and thus amplify the characteristics of the repiquetes? The answer to this question is mainly limited by the lack of measurement of environmental variables in the vertical of the region that could be contrasted and, thus, improve the outputs provided by models. For example, there are no radiosonde records in the entire study area and towards 3°N (Zhou et al., 2021).

Overall, high values of moisture convergence induced by an increase of anomaly moisture flux and precipitations over the northern Marañón and Ucayali basins were the principal characteristics that defined the initiation and the risk magnitude of repiquetes. This spatial pattern of rainfall anomalies agrees well with the propagation of the convective core of the MJO in western tropical South America that is characterized by positive rainfall anomalies in the northern Marañón and Ucayali basins (particularly during the phases 8 +1 of MJO) according to Fig. 3 in Recalde-Coronel et al. (2020).

Similar to what was proposed by previous studies, the use of ensemble forecasts that feed calibrated hydrological models seems to be one of the best alternatives; it can be complemented with recent data-based models. In addition, the atmospheric patterns defined in this study for repiquetes with risk magnitude could help forecast repiquetes 6 days before the water level starts to rise at the

Tamshiyacu gauging station. These days can be used to warn farmers of potential floods and prevent the loss of seeds. Since farmers sow as the river's water level decreases, an increase in water level could remove the seeds and carry them downstream.

Hydraulic simulations showed that for the 2002 (2.34 m of risk magnitude) and 2008 (1.29 m of risk magnitude), repiquetes probably flooded 40% (estimated in 25 tons of rice) and 25% (16 tons of rice) of the available cultivation area at the initiation of repiquete, respectively. A previous study (List and Coomes, 2017) based on repiquetes registered at the Iquitos gauging station determined that the repiquete of 2002 would have flooded between 88% and 52% of silt bars in the Muyuy anabranching structure downstream of Tamshiyacu City. The 2013 shortfalls had different hazards (considering repiquete between the most important). This was estimated at 3.7 tons per farmer. The difference in flooding impacts by repiquetes between List and Coomes (2017) and this study could be related to the topographic gradient of floodplain elevations and the influence of precipitation over the Itaya River subbasin that influences the magnitude of repiquetes in the Iquitos gaging station (Itaya River).

The positive and negative trends of dry-days frequency in the southern and northern Amazon basins, respectively (Espinoza et al., 2016; Langenbrunner et al., 2019; Wongchuig-Correa et al., 2017), and projections of increment in precipitation over the northwestern Amazon basin (Sorribas et al., 2016; Zulkafli et al., 2016) could affect the frequency of repiquete events. However, deforestation in the Amazon influences rainfall reduction over the basin (Sierra et al., 2022; Staal et al., 2020), thus affecting the role of forest transpiration that produces around one-third of Amazon rainfall (Staal et al., 2018). Similarly, deforestation could affect the shallow convection produced by forests that moisten and destabilize the atmosphere before the arrival of the Intertropical Convergence Zone (ITCZ) (Wright et al., 2017). Prior work (Ronchail et al., 2018) indicated probably better conditions for riparian agriculture based on the positive trend of the low-water period and the negative trend of low-water level (Espinoza et al., 2011; Lavado-Casimiro et al., 2012; Wongchuig-Correa et al., 2017), which would increase the available area for agriculture when the water level starts to drop. However, it is still unclear how future changes in climate variability could affect the occurrence of repiquetes. This unsolved question could be answered in future research.

Flooded extent areas by repiquetes were estimated using the 1D HEC-RAS model instead of the 2D HEC-RAS version considering the facility of application, the reduced time simulation, the morphology of the Amazon River reach (straight reach without complex morphological structures), and the hydrographs of repiquetes (less than the extreme flows). Similar results of flood extent in floodplains are obtained between the 1D and 2D models (Alzahrani, 2017; Horritt and Bates, 2002), considering the extension of the floodplains and the limitations of the model version. However, due to the complex meandering of other reaches of the Amazon River, one must evaluate the application of the 2D model (Trigg et al., 2009) to simulate repiquete events.

A limitation to extrapolating this study's findings is that the flooded area results are subject to the topography of the cultivation area and their changes throughout the length of the Amazon River. Additional topography studies are needed to replicate this study in another river area. However, considering the hydraulic gradient, the flooded risk associated with water level and peak elevations of repiquetes can be used in another part of the Amazon River. To apply this methodology in another river, such as the Ucayali River, one must also obtain daily water level time series and grid precipitation data.

5. Conclusions

This study investigates the flooding risk of croplands produced by reversal water levels, known as repiquetes, in the Peruvian Tamshiyacu gauging station in the western Amazon basin. Field survey data, satellite-based data, statistical analysis, hydraulic simulations, and atmospheric assessments were used to understand the risk of repiquete flooding. The results indicate that floodplain agriculture areas located between 83 and 88 masl in our studied region are impacted by the occurrence of repiquetes at 1.8 events per year on average (1996–2018). However, the flooding risk is particularly high for the low elevation range below 85.31 masl. Thus, percentiles of peak elevations of repiquetes have been determined in floodplain areas. While terrain elevations between 85.31 and 87.00 masl have a reduced flooding risk of 0.35 per year, elevations between 87.00 and 88.00 masl (corresponding to 43% of the total area) are unaffected by repiquetes. Extreme repiquetes that occurred in 2002 and 2008 are analyzed in more detail in this study. These extreme events could seriously affect farmland by flooding up to 40% of the available area at the initiation of the event for up to 42 days. Extreme events are primarily related to high precipitation rates over the northern Marañón basin (including the Andes-Amazon transition zone) and the northern Ucayali basin. Changes in the low-level wind circulations intensify the atmospheric moisture flux and its convergence over these regions producing extreme precipitations through the six previous days.

These results could be a tool for farmers in the region to select seed rice varieties (short or large vegetative period) as a function of the terrain elevation and the potential risk of flooding by repiquetes identified in this study. Considering that 43% of the area is unaffected by flooding repiquetes, farmers could use large vegetative period seeds in this area to improve productivity. In addition, farmers could be trained to identify flood risk zones on the ground while the water level is falling, thus referencing the water level measured at the gauging station. Therefore, disseminating and communicating these findings to the local farming community is a key challenge for the scientific community to consider.

The study was limited by a lack of information on daily water levels and the low density of gauging stations in the western Amazon basin. There were also challenges in obtaining terrain elevation with high accuracy due to poor accessibility. In addition, the relationship between repiquetes and climatological forcing brings up the question of how climatic change will affect these repiquetes events, which is currently unclear. Finally, overcoming these limitations could help to establish an early warning system based on remote sensing precipitation and real-time gauging stations that identify repiquetes before they reach the agricultural floodplains.

CRediT authorship contribution statement

Jonathan Valenzuela: Conceptualization, Methodology, Software, Validation, Formal analysis, Investigation, Data curation, Writing – original draft, Writing – review & editing, Visualization. **Manuel Figueroa**: Conceptualization, Methodology, Software, Validation, Formal analysis, Investigation, Resources, Data curation, Writing – original draft, Writing – review & editing, Visualization. **Elisa Armijos, Jhan-Carlo Espinoza**: Conceptualization, Methodology, Formal analysis, Writing – original draft, Writing – review & editing. **Sly Wongchuig, John J. Ramirez-Avila**: Methodology, Formal analysis, Writing – original draft, Writing – review & editing.

Declaration of Competing Interest

The authors declare the following financial interests/personal relationships which may be considered as potential competing interests. Elisa Armijos reports financial support was provided by Fondo Nacional de Desarrollo Científico y Tecnológico.

Data availability

Data will be made available on request.

Acknowledgments

This research has been supported by the N° 412–2019-FONDECYT/BM Project. JCE and SW were supported by the French AMANECER-MOPGA project funded by ANR and IRD (ref. ANR18-MPGA-0008). Special thanks to SO-Hybam for the hydrological series provided for this study and the Dirección Zonal 8 - Servicio Nacional de Meteorología e Hidrología (SENAMHI) of Perú. We are also grateful to Pascal Fraizy (1960–2021) for his contribution to this paper and his spirit of sharing his knowledge in search of the improvement of hydrological science in the Amazon River. Atmospheric analysis was done in Python using xarray (https://github.com/pydata/xarray).

Appendix A. Supporting information

Supplementary data associated with this article can be found in the online version at doi:10.1016/j.ejrh.2023.101428.

References

Alzahrani, A.S., 2017, Application of Two-Dimensional Hydraulic Modeling in Riverine Systems Using HEC-RAS.

Armijos, E., Crave, A., Vauchel, P., Fraizy, P., Santini, W., Moquet, J.-S., Arevalo, N., Carranza, J., Guyot, J.-L., 2013. Suspended sediment dynamics in the Amazon River of Peru. J. South Am. Earth Sci. 44, 75–84. https://doi.org/10.1016/j.jsames.2012.09.002.

Armijos, E., Crave, A., Espinoza, J.C., Filizola, N., Espinoza-Villar, R., Ayes, I., Fonseca, P., Fraizy, P., Gutierrez, O., Vauchel, P., Camenen, B., Martiınez, J.M., Dos Santos, A., Santini, W., Cochonneau, G., Guyot, J.L., 2020. Rainfall control on Amazon sediment flux: synthesis from 20 years of monitoring. Environ. Res Commun. 2, 051008 https://doi.org/10.1088/2515-7620/AB9003.

Callède, J., Cochonneau, G., Alves, F.V., Guyot, J.-L., Guimarães, V.S., De Oliveira, E., 2010. Les apports en eau de l'Amazone à l'Océan Atlantique. Rev. Des. Sci. De. l'eau 23, 247–273. https://doi.org/10.7202/044688ar.

Campozano, L., Trachte, K., Célleri, R., Samaniego, E., Bendix, J., Albuja, C., Mejia, J.F., 2018. Climatology and Teleconnections of Mesoscale Convective Systems in an Andean Basin in Southern Ecuador: The Case of the Paute Basin. Adv. Meteorol. 2018, 1–13. https://doi.org/10.1155/2018/4259191.

Chavez, S.P., Takahashi, K., 2017. Orographic rainfall hot spots in the Andes-Amazon transition according to the TRMM precipitation radar and in situ data. J. Geophys. Res.: Atmospheres 122, 5870–5882. https://doi.org/10.1002/2016JD026282.

Chibnik, M., 1994. Risky Rivers: The Economics and Politics of Floodplain Farming in Amazonia. University of Arizona Press,, Tucson.

Collischonn, W., Allasia, D., Da Silva, B.C., Tucci, C.E., 2007. The MGB-IPH model for large-scale rainfall–runoff modelling. Hydrol. Sci. J. 878–895.

Coomes, O.T., Lapointe, M., Templeton, M., List, G., 2016. Amazon river flow regime and flood recessional agriculture: Flood stage reversals and risk of annual crop loss. J. Hydrol. (Amst.) 539, 214–222. https://doi.org/10.1016/J.JHYDROL.2016.05.027.

Costa, M.H., Borma, L.S., Espinoza, J.-C., Macedo, M., Marengo, J.A., Marra, D.M., Ometto, J.P., Gatti, L.V., 2021. Chapter 5: The Physical hydroclimate system of the Amazon, in: Amazon Assessment Report 2021. UN Sustain. Dev. Solut. Netw. (SDSN). https://doi.org/10.55161/HTSD9250.

Dee, D.P., Uppala, S.M., Simmons, A.J., Berrisford, P., Poli, P., Kobayashi, S., Andrae, U., Balmaseda, M.A., Balsamo, G., Bauer, P., Bechtold, P., Beljaars, A.C.M., van de Berg, L., Bidlot, J., Bormann, N., Delsol, C., Dragani, R., Fuentes, M., Geer, A.J., Haimberger, L., Healy, S.B., Hersbach, H., Hólm, E.V., Isaksen, L., Kållberg, P., Köhler, M., Matricardi, M., McNally, A.P., Monge-Sanz, B.M., Morcrette, J.-J., Park, B.-K., Peubey, C., de Rosnay, P., Tavolato, C., Thépaut, J.-N., Vitart, F., 2011. The ERA-Interim reanalysis: configuration and performance of the data assimilation system. Q. J. R. Meteorol. Soc. 137, 553–597. https://doi.org/10.1002/qj.828.

Denevan, W.M., 1996. A Bluff Model of Riverine Settlement in Prehistoric Amazonia. Ann. Assoc. Am. Geogr. 86, 654–681. https://doi.org/10.1111/j.1467-8306.1996.tb01771.x.

DIA, 2011, Dirección de Información Agraria. Arroz. Iquitos.

Espinoza, J.C., Ronchail, J., Guyot, J.L., Cochonneau, G., Naziano, F., Lavado, W., De Oliveira, E., Pombosa, R., Vauchel, P., 2009. Spatio-temporal rainfall variability in the Amazon basin countries (Brazil, Peru, Bolivia, Colombia, and Ecuador. Int. J. Climatol. 29, 1574–1594. https://doi.org/10.1002/joc.1791.

Espinoza, J.C., Ronchail, J., Guyot, J.L., Junquas, C., Vauchel, P., Lavado, W., Drapeau, G., Pombosa, R., 2011. Climate variability and extreme drought in the upper Solimões River (western Amazon Basin): Understanding the exceptional 2010 drought. Geophys Res Lett. 38 https://doi.org/10.1029/2011GL047862.

Espinoza, J.C., Lengaigne, M., Ronchail, J., Janicot, S., 2012. Large-scale circulation patterns and related rainfall in the Amazon Basin: a neuronal networks approach. Clim. Dyn. 38, 121–140. https://doi.org/10.1007/s00382-011-1010-8.

Espinoza, J.C., Ronchail, J., Frappart, F., Lavado, W., Santini, W., Guyot, J.L., 2013. The Major Floods in the Amazonas River and Tributaries (Western Amazon Basin) during the 1970–2012 Period: A Focus on the 2012 Flood. J. Hydrometeorol. 14, 1000–1008. https://doi.org/10.1175/JHM-D-12-0100.1.

Espinoza, J.C., Chavez, S., Ronchail, J., Junquas, C., Takahashi, K., Lavado, W., 2015. Rainfall hotspots over the southern tropical Andes: Spatial distribution, rainfall intensity, and relations with large-scale atmospheric circulation. Water Resour. Res 51, 3459–3475. https://doi.org/10.1002/2014WR016273.

Espinoza, J.C., Segura, H., Ronchail, J., Drapeau, G., Gutierrez-Cori, O., 2016. Evolution of wet-day and dry-day frequency in the western Amazon basin: Relationship with atmospheric circulation and impacts on vegetation. Water Resour. Res 52, 8546–8560. https://doi.org/10.1002/2016WR019305.

Espinoza, J.C., Garreaud, R., Poveda, G., Arias, P.A., Molina-Carpio, J., Masiokas, M., Viale, M., Scaff, L., 2020. Hydroclimate of the Andes Part I: Main Climatic Features. Front Earth Sci. (Lausanne) 8. https://doi.org/10.3389/feart.2020.00064.

Espinoza, J.C., Arias, P.A., Moron, V., Junquas, C., Segura, H., Sierra-Pérez, J.P., Wongchuig, S., Condom, T., 2021. Recent changes in the atmospheric circulation patterns during the dry-to-wet transition season in south tropical South America (1979-2020): Impacts on precipitation and fire season. J. Clim. 1–56. https://doi.org/10.1175/JCLI-D-21-0303.1.

Figueroa, M., Armijos, E., Espinoza, J.C., Ronchail, J., Fraizy, P., 2020. On the relationship between reversal of the river stage (repiquetes), rainfall and low-level wind regimes over the western Amazon basin. J. Hydrol. Reg. Stud. 32, 100752 https://doi.org/10.1016/J.EJRH.2020.100752.

Figueroa, S., Nobre, C., 1990. Precipitation distribution over central and western tropical South America. Climanálise 5, 36–45.

Foley, J.A., Asner, G.P., Costa, M.H., Coe, M.T., DeFries, R., Gibbs, H.K., Howard, E.A., Olson, S., Patz, J., Ramankutty, N., Snyder, P., 2007. Amazonia revealed: forest degradation and loss of ecosystem goods and services in the Amazon Basin. Front Ecol. Environ. 5, 25–32. https://doi.org/10.1890/1540-9295(2007)5[25:ARFDAL]2.0.CO;2.

Funk, C., Peterson, P., Landsfeld, M., Pedreros, D., Verdin, J., Shukla, S., Husak, G., Rowland, J., Harrison, L., Hoell, A., Michaelsen, J., 2015. The climate hazards infrared precipitation with stations—a new environmental record for monitoring extremes. Sci. Data 2, 150066. https://doi.org/10.1038/sdata.2015.66.

González-Rojí, S.J., Messmer, M., Raible, C.C., Stocker, T.F., 2022. Sensitivity of precipitation in the highlands and lowlands of Peru to physics parameterization options in WRFV3.8.1. Geosci. Model Dev. 15, 2859–2879. https://doi.org/10.5194/gmd-15-2859-2022.

Gorenstein, S., 2023, Government Rationality and Risk Production: Case Study from River Communities in Peru. Preprints (Basel).

Hiraoka, M., 1985. Floodplain Farming in the Peruvian Amazon. Geogr. Rev. Jpn., Ser. B. 58, 1–23. https://doi.org/10.4157/grj1984b.58.1.

Horritt, M.S., Bates, P.D., 2002. Evaluation of 1D and 2D numerical models for predicting river flood inundation. J. Hydrol. (Amst.) 268, 87–99. https://doi.org/10.1016/S0022-1694(02)00121-X.

INIA, 2001, Instituto Nacional de Innovación Agraria. Variedad Capirona INIA.

INIA, 2005, Instituto Nacional de Innovación Agraria. Arroz INIA 506 - JAR I.

INIA, 2007, Instituto Nacional de Innovación Agraria. Arroz INIA 505 - Ecoarroz.

INIA, 2010, Instituto Nacional de Innovación Agraria. Arroz INIA 509 - La Esperanza.

Jakovac, C.C., Dutrieux, L.P., Siti, L., Peña-Claros, M., Bongers, F., 2017. Spatial and temporal dynamics of shifting cultivation in the middle-Amazonas river: Expansion and intensification. PLoS One 12, e0181092. https://doi.org/10.1371/journal.pone.0181092.

Jardim, C.M., Nardoto, G.B., de Lima, A.C.B., de Jesus Silva, R., Schor, T., de Oliveira, J.A., Martinelli, L.A., 2020. The influence of seasonal river flooding in food consumption of riverine dwellers in the central Amazon region: an isotopic approach. Archaeol. Anthr. Sci. 12, 205. https://doi.org/10.1007/s12520-020-01172-5.

Jones, C., Carvalho, L.M.V., 2002. Active and Break Phases in the South American Monsoon System. J. Clim. 15, 905–914. https://doi.org/10.1175/1520-0442(2002)015<0905:AABPIT>2.0.CO;2.

Junquas, C., Takahashi, K., Condom, T., Espinoza, J.-C., Chavez, S., Sicart, J.-E., Lebel, T., 2018. Understanding the influence of orography on the precipitation diurnal cycle and the associated atmospheric processes in the central Andes. Clim. Dyn. 50, 3995–4017. https://doi.org/10.1007/s00382-017-3858-8.

Labarta, R., White, D., Leguía, E., Guzmán, W., Soto, J., 2007. La agricultura en la Amazonia ribereña del río Ucayali: ¿una zona productiva pero poco rentable? Acta Amaz. 37, 177–186. https://doi.org/10.1590/S0044-59672007000200002.

Langenbrunner, B., Pritchard, M.S., Kooperman, G.J., Randerson, J.T., 2019. Why Does Amazon Precipitation Decrease When Tropical Forests Respond to Increasing CO_2? Earths Future 7, 450–468. https://doi.org/10.1029/2018EF001026.

Laraque, A., Ronchail, J., Cochonneau, G., Pombosa, R., Guyot, J.L., 2007. Heterogeneous distribution of rainfall and discharge regimes in the Ecuadorian Amazon Basin. J. Hydrometeorol. 8, 1364–1381. https://doi.org/10.1175/2007JHM784.1.

Lavado-Casimiro, W., Ronchail, J., Labat, D., Espinoza, J.C., Guyot, J.L., 2012. Basin-scale analysis of rainfall and runoff in Peru (1969–2004): Pacific, Titicaca and Amazonas drainages. Hydrol. Sci. J. 57, 625–642. https://doi.org/10.1080/02626667.2012.672985.

Lavado-Casimiro, W., Labat, D., Ronchail, J., Espinoza, J.C., Guyot, J.L., 2013. Trends in rainfall and temperature in the Peruvian Amazon-Andes basin over the last 40 years (1965-2007). Hydrol. Process 27, 2944–2957. https://doi.org/10.1002/hyp.9418.

List, G., Coomes, O., 2019. Repiquetes y riesgo en el cultivo de arroz en la llanura inundable del río Amazonas cerca de Iquitos, Perú. Folia Amaz. 28, 19–32. https://doi.org/10.24841/FA.V28I1.466.

List, G., Coomes, O.T., 2017. Natural hazards and risk in rice cultivation along the upper Amazon River. Nat. Hazards 2017 87 1 (87), 165–184. https://doi.org/10.1007/S11069-017-2758-X.

Marengo, J.A., Soares, W.R., Saulo, C., Nicolini, M., 2004. Climatology of the Low-Level Jet East of the Andes as Derived from the NCEP–NCAR Reanalyses: Characteristics and Temporal Variability. J. Clim. 17, 2261–2280. https://doi.org/10.1175/1520-0442(2004)017<2261:COTLJE>2.0.CO;2.

Mayta, V.C., Ambrizzi, T., Espinoza, J.C., Silva Dias, P.L., 2019. The role of the Madden-Julian oscillation on the Amazon Basin intraseasonal rainfall variability. Int. J. Climatol. 39, 343–360. https://doi.org/10.1002/joc.5810.

Mendoza, A., Abad, J.D., Frias, C.E., Ortals, C., Paredes, J., Montoro, H., Vizcarra, J., Simon, C., Soto-Cortés, G., 2016. Planform dynamics of the Iquitos anabranching structure in the Peruvian Upper Amazon River. Earth Surf. Process Land. 41, 961–970. https://doi.org/10.1002/ESP.3911.

Paccini, L., Espinoza, J.C., Ronchail, J., Segura, H., 2018. Intra-seasonal rainfall variability in the Amazon basin related to large-scale circulation patterns: a focus on western Amazon-Andes transition region. Int. J. Climatol. 38, 2386–2399. https://doi.org/10.1002/joc.5341.

Pontes, P.R.M., Fan, F.M., Fleischmann, A.S., de Paiva, R.C.D., Buarque, D.C., Siqueira, V.A., Jardim, P.F., Sorribas, M.V., Collischonn, W., 2017. MGB-IPH model for hydrological and hydraulic simulation of large floodplain river systems coupled with open source GIS. Environ. Model. Softw. 94, 1–20. https://doi.org/10.1016/J.ENVSOFT.2017.03.029.

Poveda, G., Jaramillo, L., Vallejo, L.F., 2014. Seasonal precipitation patterns along pathways of South American low-level jets and aerial rivers. Water Resour. Res 50, 98–118. https://doi.org/10.1002/2013WR014087.

Recalde-Coronel, G.C., Zaitchik, B., Pan, W.K., 2020. Madden–Julian oscillation influence on sub-seasonal rainfall variability on the west of South America. Clim. Dyn. 54, 2167–2185. https://doi.org/10.1007/s00382-019-05107-2.

Rehbein, A., Ambrizzi, T., Mechoso, C.R., 2018. Mesoscale convective systems over the Amazon basin. Part I: climatological aspects. Int. J. Climatol. 38, 215–229. https://doi.org/10.1002/joc.5171.

Ronchail, J., Schor, T., Espinoza, J.C., Sabot, M., Pinheiro, H., Filizola, N., Gomez, P., Drapeau, G., Michot, V., Guyot, J.L., Martinez, J.M., Sultan, B., 2016, Hydrologie et production agricole dans le nord-ouest de l'Amazonie. http://journals.openedition.org/bagf 93, 270–286. https://doi.org/10.4000/BAGF.1168.

Ronchail, J., Espinoza, J.C., Drapeau, G., Sabot, M., Cochonneau, G., Schor, T., 2018. The flood recession period in Western Amazonia and its variability during the 1985–2015 period. J. Hydrol. Reg. Stud. 15, 16–30. https://doi.org/10.1016/J.EJRH.2017.11.008.

Satyamurty, P., Nobre, C.A., Silva Dias, P.L., 1998. South America. In: Meteorology of the Southern Hemisphere. American Meteorological Society, Boston, MA, pp. 119–139. https://doi.org/10.1007/978-1-935704-10-2_5.

Segura, H., Junquas, C., Espinoza, J.C., Vuille, M., Jauregui, Y.R., Rabatel, A., Condom, T., Lebel, T., 2019. New insights into the rainfall variability in the tropical Andes on seasonal and interannual time scales. Clim. Dyn. 53, 405–426. https://doi.org/10.1007/s00382-018-4590-8.

Sierra, J.P., Junquas, C., Espinoza, J.C., Segura, H., Condom, T., Andrade, M., Molina-Carpio, J., Ticona, L., Mardoñez, V., Blacutt, L., Polcher, J., Rabatel, A., Sicart, J. E., 2022. Deforestation impacts on Amazon-Andes hydroclimatic connectivity. Clim. Dyn. 58, 2609–2636. https://doi.org/10.1007/s00382-021-06025-y.

Sioli, H., 1984, Unifying principles of Amazonian landscape ecology and their implications. pp. 615–625. https://doi.org/10.1007/978–94-009–6542-3_24.
Sorribas, M.V., Paiva, R.C.D., Melack, J.M., Bravo, J.M., Jones, C., Carvalho, L., Beighley, E., Forsberg, B., Costa, M.H., 2016. Projections of climate change effects on discharge and inundation in the Amazon basin. Clim. Change 136, 555–570. https://doi.org/10.1007/s10584-016-1640-2.
Staal, A., Tuinenburg, O.A., Bosmans, J.H.C., Holmgren, M., van Nes, E.H., Scheffer, M., Zemp, D.C., Dekker, S.C., 2018. Forest-rainfall cascades buffer against drought across the Amazon. Nat. Clim. Chang 8, 539–543. https://doi.org/10.1038/s41558-018-0177-y.
Staal, A., Flores, B.M., Aguiar, A.P.D., Bosmans, J.H.C., Fetzer, I., Tuinenburg, O.A., 2020. Feedback between drought and deforestation in the Amazon. Environ. Res. Lett. 15, 044024 https://doi.org/10.1088/1748-9326/ab738e.
Trachte, K., 2018. Atmospheric Moisture Pathways to the Highlands of the Tropical Andes: Analyzing the Effects of Spectral Nudging on Different Driving Fields for Regional Climate Modeling. Atmosphere (Basel) 9, 456. https://doi.org/10.3390/atmos9110456.
Trigg, M.A., Wilson, M.D., Bates, P.D., Horritt, M.S., Alsdorf, D.E., Forsberg, B.R., Vega, M.C., 2009. Amazon flood wave hydraulics. J. Hydrol. (Amst.) 374, 92–105. https://doi.org/10.1016/j.jhydrol.2009.06.004.
Vera, C., Higgins, W., Amador, J., Ambrizzi, T., Garreaud, R., Gochis, D., Gutzler, D., Lettenmaier, D., Marengo, J., Mechoso, C.R., Nogues-Paegle, J., Dias, P.L.S., Zhang, C., 2006. Toward a Unified View of the American Monsoon Systems. J. Clim. 19, 4977–5000. https://doi.org/10.1175/JCLI3896.1.
Wang, H., Fu, R., 2002. Cross-equatorial flow and seasonal cycle of precipitation over South America. J. Clim. 15, 1591–1608. https://doi.org/10.1175/1520-0442(2002)015<1591:CEFASC>2.0.CO;2.
WinklerPrins, A.M.G.A., 2022. Recent seasonal floodplain-upland migration along the lower Amazon River, Brazil. Geogr. Rev. 92, 415–431.
Wongchuig-Correa, S., de Paiva, R.C.D., Espinoza, J.C., Collischonn, W., 2017. Multi-decadal Hydrological Retrospective: Case study of Amazon floods and droughts. J. Hydrol. (Amst.) 549, 667–684. https://doi.org/10.1016/j.jhydrol.2017.04.019.
Wright, J.S., Fu, R., Worden, J.R., Chakraborty, S., Clinton, N.E., Risi, C., Sun, Y., Yin, L., 2017. Rainforest-initiated wet season onset over the southern Amazon. Proc. Natl. Acad. Sci. 114, 8481–8486. https://doi.org/10.1073/pnas.1621516114.
Zhou, C., Wang, J., Dai, A., Thorne, P.W., 2021. A new approach to homogenize global subdaily radiosonde temperature data from 1958 to 2018. J. Clim. 34, 1163–1183. https://doi.org/10.1175/JCLI-D-20-0352.1.
Zubieta, R., Getirana, A., Espinoza, J.C., Lavado, W., 2015. Impacts of satellite-based precipitation datasets on rainfall–runoff modeling of the Western Amazon basin of Peru and Ecuador. J. Hydrol. (Amst.) 528, 599–612. https://doi.org/10.1016/j.jhydrol.2015.06.064.
Zulkafli, Z., Buytaert, W., Manz, B., Rosas, C.V., Willems, P., Lavado-Casimiro, W., Guyot, J.-L., Santini, W., 2016. Projected increases in the annual flood pulse of the Western Amazon. Environ. Res. Lett. 11, 014013 https://doi.org/10.1088/1748-9326/11/1/014013.